

FILE COPY

4

OFFICE OF NAVAL RESEARCH

Contract N00014-87-K-0494

R&T Code 400X027YIP

Technical Report No. 4

Molecular Dynamics Study of the Primitive Model of
1-3 Electrolyte Studies

by

S.-H. Suh, L. Mier-y-Teran, H. S. White, and H. T. Davis

Prepared for Publication in the
Chemical Physics

University of Minnesota
Department of Chemical Engineering and Materials Science
Minneapolis, MN 55455

July, 1989

Reproduction in whole or in part is permitted for any purpose of the United States
Government.

This document has been approved for public release and sale; its distribution is unlimited.

DTIC
ELECTE
AUG 22 1989
S & E D

89 8-22 013

AD-A211 653

REPORT DOCUMENTATION PAGE

1a. REPORT SECURITY CLASSIFICATION Unclassified		1b. RESTRICTIVE MARKINGS	
2a. SECURITY CLASSIFICATION AUTHORITY		3. DISTRIBUTION/AVAILABILITY OF REPORT	
2b. DECLASSIFICATION/DOWNGRADING SCHEDULE		Unclassified/Unlimited	
4. PERFORMING ORGANIZATION REPORT NUMBER(S) ONR Technical Report 4		5. MONITORING ORGANIZATION REPORT NUMBER(S)	
6a. NAME OF PERFORMING ORGANIZATION Dept of Chemical Engineering and Materials Science	6b. OFFICE SYMBOL (If applicable) Code 1113	7a. NAME OF MONITORING ORGANIZATION Office of Naval Research	
6c. ADDRESS (City, State, and ZIP Code) University of Minnesota Minneapolis, MN 55455		7b. ADDRESS (City, State, and ZIP Code) 800 North Quincy Street Arlington, VA 22217	
8a. NAME OF FUNDING/SPONSORING ORGANIZATION Office of Naval Research	8b. OFFICE SYMBOL (If applicable)	9. PROCUREMENT INSTRUMENT IDENTIFICATION NUMBER Contract No. N00014-87-R-0494	
8c. ADDRESS (City, State, and ZIP Code) 800 North Quincy Street Arlington, VA 22217-5000		10. SOURCE OF FUNDING NUMBERS	
		PROGRAM ELEMENT NO.	PROJECT NO.
		TASK NO.	WORK UNIT ACCESSION NO.
11. TITLE (Include Security Classification) Molecular Dynamics Study of the Primitive Model of 1-3 Electrolyte Study			
12. PERSONAL AUTHOR(S) S.-H. Suh, L. Mier-y-Teran, H.S. White, and H.T. Davis			
13a. TYPE OF REPORT Technical	13b. TIME COVERED FROM _____ TO _____	14. DATE OF REPORT (Year, Month, Day)	15. PAGE COUNT
16. SUPPLEMENTARY NOTATION prepared for publication in the Chemical Physics			
17. COSATI CODES		18. SUBJECT TERMS (Continue on reverse if necessary and identify by block number)	
FIELD	GROUP	SUB-GROUP	
19. ABSTRACT (Continue on reverse if necessary and identify by block number) Molecular dynamics simulations at constant temperature have been carried out for the primitive model of 1-3 electrolyte solutions. Thermodynamics, pair distribution functions, and self-diffusion coefficients were computed to examine the electrostatic effects on the structural and dynamical properties. The simulation results were used to evaluate various theoretical equations, namely, the exponential form of Debye-Huckel theory, the mean spherical approximation, and the hypernetted chain approximation. As has been observed for symmetrical electrolytes, the latter turns out to be the best approximation. For asymmetrically charged 1-3 electrolytes, it was found that ionic aggregation significantly influenced the dynamical properties of electrolytes. Coherent motion between highly charged negative ions and positive ions surrounding them was deduced from the time dependence of the velocity autocorrelation functions, particularly at concentrations between 0.4 and 4 total molar.			
20. DISTRIBUTION/AVAILABILITY OF ABSTRACT <input checked="" type="checkbox"/> UNCLASSIFIED/UNLIMITED <input type="checkbox"/> SAME AS RPT. <input type="checkbox"/> OTIC USERS		21. ABSTRACT SECURITY CLASSIFICATION Unclassified	
22a. NAME OF RESPONSIBLE INDIVIDUAL Henry S. White		22b. TELEPHONE (Include Area Code) (612) 625-6995	22c. OFFICE SYMBOL

**Molecular Dynamics Study of the Primitive Model
of 1-3 Electrolyte Solutions**

by

S.-H. Suh, L. Mier-y-Teran*, H. S. White, and H. T. Davis

Department of Chemical Engineering and Materials Science,
University of Minnesota, Minneapolis, MN 55455

Submitted to Chemical Physics (June, 1989).

Accession For	
NTIS GRA&I	<input checked="checked" type="checkbox"/>
DTIC TAB	<input type="checkbox"/>
Unannounced	<input type="checkbox"/>
Justification	
By	
Distribution/	
Availability Codes	
Dist	Avail. and/or Special
A-1	

* On sabbatical leave from Departamento de Fisica, Universidad Autonoma Metropolitana-Iztapalapa, Apartado Postal 55-534, 09340 Mexico, D.F., Mexico

Abstract

Molecular dynamics simulations at constant temperature have been carried out for the primitive model of 1-3 electrolyte solutions. Thermodynamics, pair distribution functions, and self-diffusion coefficients were computed to examine the electrostatic effects on the structural and dynamical properties. The simulation results were used to evaluate various theoretical equations, namely, the exponential form of Debye-Huckel theory, the mean spherical approximation, and the hypernetted chain approximation. As has been observed for symmetrical electrolytes, the latter turns out to be the best approximation. For asymmetrically charged 1-3 electrolytes, it was found that ionic aggregation significantly influenced the dynamical properties of electrolytes. Coherent motion between highly charged negative ions and positive ions surrounding them was deduced from the time dependence of the velocity autocorrelation functions, particularly at concentrations between 0.4 and 4 total molar.

1. Introduction

During the last couple of decades much progress has been made in our understanding and interpretation of the physical properties of electrolyte solutions. A number of different theoretical approximations [1-7] have been used to evaluate the thermodynamic and structural properties of bulk electrolytes. One of the simplest but most commonly used models in these theoretical approaches is the so-called "primitive model electrolyte solution" [1,2], in which the charged hard-sphere ions are immersed in a continuum solvent represented only as a uniform dielectric constant of the medium.

Reliable and unambiguous results, in turn, have become increasingly necessary to eliminate any underlying uncertainties involved in theoretical approximations. However, the present level of modeling, particularly the use of a solvent continuum assumption, is far too crude to allow the direct comparison with real laboratory experiment. Consequently, machine experiments (computer simulations), which provide essentially "exact" experimental data for precisely defined model systems, have proven to be an extremely useful diagnostic tool to investigate such systems. The great advantage of computer simulations over experiment lies in the possibility of obtaining detailed physical information, which may be very difficult or impossible to realize in the laboratory. The best known example is the measurement of pair distribution functions as a function of distance at the molecular level.

There are in general two classes of computer experiment: stochastic Monte Carlo (MC) and deterministic molecular dynamics (MD) simulations. In the MD calculations, the actual trajectories of molecules are evaluated by the numerical integration of Newton's equations of motion. In addition to static equilibrium

properties, time-dependent transport properties can be also obtained by the MD method. For the system of primitive model electrolytes, however, the discontinuous nature of hard-sphere repulsions combined with continuous electrostatic interactions introduces some technical difficulties into the traditional MD algorithm. Recently, implementations have been made to extend the MD method to the system of hard-cores with soft attractive potentials. In the work of Heyes [8] for the restricted primitive model of 1:1 electrolytes, two different forms of MD were combined. The hard-sphere collisions were allowed to take place while the forces and velocity changes due to continuous electrostatic interactions were evaluated. The agreement with the previous MC calculations was excellent even at higher concentrations.

Almost all simulations for the primitive electrolytes have been carried out using the MC simulation method [9-12]. Much of the earlier work on the MC calculations in a variety of different ensembles has been summarized by Levesque et al. [13]. Valleau and his collaborators have extensively reported the canonical and the grand canonical MC results [9] of such systems. In their studies, various theoretical approaches were also discussed and compared with the results obtained from their MC simulations. They adopted the minimum image convention to evaluate the Coulombic part of potentials for each configuration, and the resulting energy was linearly extrapolated as a function of $1/N$ to estimate the values of an infinite system. These data should be accepted with some care because the method with as few as 200 ions the method could yield results depending on system size. This is particularly true for higher concentrations and for higher charged systems. Explicit results for osmotic pressure were not published in the previous works.

In the MD simulations, better statistics can be achieved. For instance, in

order to calculate the virial contribution to the equation of state for the hard-core system, the MC computations require an accurate estimation of pair distribution functions at the contact point [14]. For the system of ionic solutions, pair functions may change rapidly near contact distances due to the formation of ionic aggregates (see Fig. 4a). The extrapolation of pair functions to the contact value lead to large uncertainties in this case of ionic solutions. For this reason the MC results for osmotic pressure coefficients are known to be less certain than those for energy calculations.

In the present paper, we report computer simulation results for the asymmetrically charged system of 1-3 electrolyte solutions via molecular dynamics simulation techniques. This asymmetric system is of special interest because it provides a strong test of the applicability of approximate theories available in the literature. Computational details of the method employed here are discussed in the next section. In section 3, the thermodynamic and structural properties obtained from our MD simulations are compared with various theoretical predictions, namely, the exponential form of Debye-Huckel theory [9,15], the mean spherical approximation [3], and the hypernetted chain approximation [4]. We also report in this section the dynamical properties including the velocity autocorrelation functions and the self-diffusion coefficients. The dynamical properties of the primitive model electrolytes are of course not comparable to those of electrolyte solutions since solvent dynamics are totally absent in this model. However, the results are an inexpensive by-product of the simulation and should be useful for testing the approximate theories of transport in charged systems (e.g., plasmas and molten salts).

2. Model and Computations

The MD calculations were carried out with a system containing 216 charged hard-spheres with equal diameter, d , of 0.425 nm and mass, m , of 100 a.m.u. (There are 162 cations with charge +1 and 54 anions with charge -3.) Usual periodic boundary conditions were applied in a cubic fundamental cell to approximate an infinite system.

The pair potential energy between ions i and j is (in S.I. units)

$$U_{ij}(r) = \begin{cases} \infty & \text{if } x < d \\ \frac{z_i z_j q^2}{4\pi \epsilon_0 \epsilon_r r} & \text{if } x > d, \end{cases} \quad (1)$$

where z_i and z_j are the valence of ion i and j , and q is the unit of electronic charge. ϵ_r is the uniform dielectric constant of the medium relative to the permittivity of free space, ϵ_0 . As used in most other studies, the relative dielectric constant, ϵ_r , was chosen to be 78.356 corresponding to those for water at room temperature, 298.16 K.

The long-ranged interactions in ionic systems give a configurational energy that converges slowly with the increasing system size. Use of a spherical cut-off or a minimum image convention has shown to be inappropriate, particularly for highly charged dense systems [16]. The resulting configurational energy for such systems must take account for the ion pairs not only with the nearest images in a fundamental cell but also with all images in other periodic cells. The Coulombic potentials or forces, in this study, were calculated using the Ewald sum technique [17], which is a well-known method for evaluating the electrostatic interactions in ionic crystals.

The Ewald transformation is expressed by two convergent sums. One in real space of a short-ranged potential, U_n ,

$$U_n = \frac{1}{2} \sum_{i=1}^N \sum_{j=1}^N \sum_n \frac{z_i z_j q^2}{4\pi \epsilon_o \epsilon_r} \frac{\text{erfc}(\alpha r_{ij,n})}{r_{ij,n}}, \quad (2a)$$

and the other in reciprocal lattice space of periodic Fourier domains, U_h ,

$$U_h = \frac{1}{2\pi L} \sum_{i=1}^N \sum_{j=1}^N \sum_{h \neq 0} \frac{z_i z_j q^2}{4\pi \epsilon_o \epsilon_r} \exp\left(-\frac{\pi^2 h^2}{\alpha^2 L^2}\right) / h^2 \cos\left(\frac{2\pi}{L} \mathbf{h} \cdot \mathbf{r}_{ij}\right), \quad (2b)$$

where L is the box length, α is an arbitrary parameter, typically set to $5/L$, and erfc is the complementary error function. Note that \mathbf{h} is a reciprocal wave vector in units such that its components are integers. In the latter case of reciprocal space, the order of computations can be reduced by the method suggested by Singer [18], in which the double sum over particle i and j is simplified into two single sums over particle i . Total of 618 wave vectors were computed using a recurrence relationship of complex arithmetic to avoid repeated calculations.

The system of a hard-core repulsion with continuous attractive interactions gives rise to problems for MD computer simulations. Computational techniques for trajectory calculations are totally different between the discontinuous and the continuous MD method. In the hard-core MD program introduced in the pioneering work of Alder and Wainwright [19], the collision equations between all possible colliding pairs must be solved before advancing their trajectories. In contrast, in the MD for continuous potentials, the time evolution of phase space is followed by solving the equations of motion suitably discretized in time.

Two distinct algorithms can be combined into the same MD program by returning to the hybrid "step-by-step" approach described elsewhere [8,20,21].

The time step interval is of order of femto seconds which is very small compared to the average time between hard-sphere collisions. The first step is identical to the system of conventional continuous potentials. The system trajectories are advanced from the current positions to the next positions only under the influence of continuous forces without imposing the hard-core constraints. In this step, any possible hard-core collision occurring during a fixed time interval is ignored, and this may result in unrealistic hard-core penetration. The next step is then to check whether or not the pair distances are closer than a hard-sphere contact diameter, and the resulting configuration is resolved for the overlapping pairs. Because the time interval is so small, the majority of particles proceed without colliding with each other. When an overlap is found in a time step, the step is repeated, but this time the particle velocities are assumed to be constant. Under this assumption, the particles are advanced until the overlapping pair collides and the algebraic equations of colliding hard-spheres are used to find the postcollision positions and velocities. The algorithm then returns to the continuous potential MD sequence. This approach has been applied for the various systems of model fluids and did not show any measurable inaccuracy for the thermodynamic and transport properties of such systems [8,20,21]. A logic flow chart for this MD method is illustrated in Figure 1.

For the computational efficiency, it is appropriate to eliminate any redundant calculations and this can be done by the construction of the collider table to speed up the searching routine. Before entering the force loop in the first step, the maximum velocity was scanned to decide the maximum cut-off distance for the collider table. The table was updated at each step to ensure possible colliding pairs. Only the pairs within this maximum distance were considered to examine the colliding pairs in the next step, rather than all possible pairs.

The equations of motion were integrated using the leapfrog version of Verlet algorithm [22], and the velocities were scaled at each time step to maintain constant temperature in the manner described by Berendsen et al. [23]. In addition, the initial configurations were generated by randomly inserting particles to assist in the equilibration of the system. Configurations were aged, or equilibrated, for 6,000 steps before accumulating data and the resulting ensemble averages were obtained during the final 40,000 steps. The MD algorithm implemented here has been tested in a number of ways. When the ionic charges were assigned to a value of zero, the results faithfully reproduced the thermodynamic and transport properties of the pure hard-sphere system available in the literature [24]. The results obtained from the MD simulations for a few selected runs of 1-1 electrolytes were also compared to the MC [9] and MD [8] calculations. The good agreement with the previous data again confirmed the quality of our MD method. All production calculations were performed on a Cray-2 supercomputer at Minnesota Supercomputer Center. Extensive use was made of vectorization and optimization.

3. RESULTS AND DISCUSSION

The thermodynamic and transport properties of 1-3 electrolyte solutions obtained from the MD simulations are presented in Table 1. The range of concentration investigated here was from 0.02 Mt to 6 Mt, where Mt is the total ion concentration in units of mole per liter, but not the stoichiometric concentration, Ms. (Note that $Mt = 4 Ms = 21.6318 \text{ nd}^3$, where nd^3 is the total number density.) The self-diffusion coefficients were calculated from the integration of the velocity autocorrelation function using the Green-Kubo relations and from the slope of the mean-square displacement versus time using the Einstein equations. The two methods gave results in good agreement, typically less than 3% difference, and the self-diffusion coefficients in Table 1 are averages of the values found by the two methods. In this table, we also report the ion/ion collision frequencies in columns 7 to 9.

In Figures 2 and 3 we illustrate the concentration dependence of the reduced configurational energy, U/NkT , and the reduced osmotic pressure, PV/NkT , respectively. Also shown in these figures are the results obtained with the exponential form of Debye-Huckel theory (DHX) [9,15], the mean spherical approximation (MSA) [3], and those reported in Ref. [4] for the hypernetted chain theory (HNC). The thermodynamic properties can be expressed in terms of pair distribution functions, $g_{ij}(r)$, between ionic species i and j .

The configurational energy of the fluid is

$$\frac{U}{NkT} = \frac{2\pi n}{kT} \sum_i \sum_j \int_0^\infty U_{ij}(r) g_{ij}(r) r^2 dr, \quad (3)$$

and, the virial expression for the osmotic pressure is

$$\frac{PV}{NkT} = 1 + \frac{U}{3NkT} + \frac{2\pi nd^3}{3} \sum_i \sum_j X_i X_j g_{ij}(d), \quad (4)$$

where X_i is the mole fraction of species i and $g_{ij}(d)$ is the contact value of the pair function for species i and j .

We first focus our attention on the results obtained from the DHX theory. This simple approximation is inadequate over most of the range of the concentrations investigated in this work. The discrepancy is gradually amplified with increasing concentration. Although the poor results are observed here, we point out that for the 1-1 electrolyte system and $Mt < 2.0$ the DHX energy predictions are in reasonable qualitative agreement with previous simulation results [8]. The main failure of the DHX approximation is that it misses the structure of the pair distribution functions. The oscillatory behavior occurring at higher concentrations due to the hard-sphere exclusion volume is totally ignored in this theory. The contact values of the pair distribution functions of the DHX theory are also inaccurate.

This last point is illustrated in Figures 4a and 4b. Pair distribution functions were computed by sorting the relative pair distances into the equal radial increments of width $0.01d$. Even at the low concentration of $Mt = 0.2$ (Figure 4a), slightly more $+-$ and $++$ ion pairings at the short range of distances were found in the MD results compared with the DHX pair functions. The sharp peak near the contact point in g_{+-} indicates the strong tendency to the formation of unlike-pairs. As seen in Figure 4b ($Mt = 4.0$), however, the DHX model significantly overestimates $--$ pairings in g_{--} while the underestimation of the Coulombic attraction between unlike-pairs results in much lower value in g_{+-} . In the MC calculations for the 2-2 electrolytes [9,11], the presence of linear ion triplets was manifested by a local maximum in like-pair functions near $r = 2d$.

Similar results were observed, but, in the case of our 1-3 system, the maximum peak in g_{--} was shifted to approximately $r = 2.5d$. The salient feature displayed here is a noticeable trend to the formation of larger ionic clusterings for higher charged systems.

The MSA and HNC theories are both based on the Ornstein-Zernike integral equation along with specific closure relationships. The MSA model has a great advantage; it is the only theory that can be solved analytically for the system of charged hard-spheres [3]. As an extension to the Debye-Huckel theory, in the MSA theory, the hard-sphere oscillations due to the ion-cores have been taken into account. In the limit of point charges, the MSA becomes identical to the Debye-Huckel theory. As illustrated in Figure 2 and 3, the MSA results for the energy and for the osmotic pressure are in relatively good agreement with the MD data. However, the MSA pair distribution functions are known to be poor. Particularly for a range of low concentration, the linearized nature of the MSA model leads to the unphysical negative values among the like-pair functions as in the Debye-Huckel theory. The MSA pair functions are only symmetrically disposed around those for the hard-sphere pair function. The better agreement for pressure than for energy in the DHX model seems to be coincidental and caused by a cancellation of errors between energy and collision contributions (the second and the third term in the virial pressure in eq. (4), respectively). For $Mt = 2.0$, for instance, an underestimation in $g_{+-}(d)$ by about 30% is almost equally balanced by an overestimate in energy. The HNC results for the system of 1-3 electrolytes [4] predict the configurational energy and the osmotic pressure in very good agreement to the MD results within statistical errors. Although special iterative techniques are necessary in order to reach convergence [4], HNC theory has also shown to be successful for the 1:1 and 2:2 electrolytes [9,11].

The velocity autocorrelation functions (VACF) can provide useful insights into ion dynamics and transport. The normalized VACF is defined as a function of time, t , by

$$\text{VACF} = \frac{1}{N} \sum_{i=1}^N \langle \mathbf{v}_i(0) \cdot \mathbf{v}_i(t) \rangle / \langle \mathbf{v}_i^2(0) \rangle, \quad (5)$$

where the symbol $\langle \rangle$ denotes the average over an equilibrium ensemble. Those time correlation functions are, in principle, measurable quantities from inelastic scattering experiments.

In Figures 5a to 5c, we plot the normalized VACFs for a few selected runs to illustrate the manner in which those functions change with increasing concentration. The solid curves correspond to the VACFs for positively charged ions, VACF(+), and, respectively, the dotted curves, for negatively charged ions, VACF(-). The VACFs for lower concentration exhibit a stronger velocity autocorrelation than those for higher concentration. The primary mechanism of decay of the time correlation functions is the hard-sphere collision, in which colliding particles rapidly forget their initial velocities through successive collision. In the high concentration regime, the hard-core repulsive collisions are expected to play a dominant role in determining the dynamical properties of the system. In agreement with this, the resulting VACF(+)s exhibit the exponential behavior which characterizes the dynamics of hard-sphere fluids [24].

However, as shown by the VACF(-)s in Figure 5, there are substantial differences between the motion of the positive charges and the highly charged negative ions. The VACF(-)s decay more rapidly than the VACF(+)s. The VACF(-)s exhibit non-exponential behavior. At low or intermediate concentration, the long-ranged Coulombic potential increasingly influences the collective

motion of ionic fluids by the acceleration or retardation of velocities between colliding pairs. The electrostatic force enhances correlations between unlike-pairs, and decorrelation between like-pairs.

The most striking feature of the $VACF(-)$ s is the peculiar peak displayed in the range of intermediate concentration. The peak occurs at relatively the short time delay between 5 ps and 10 ps. At the very low concentration regime, the $VACF(-)$ decays monotonically. However, a weakly oscillatory behavior starts to emerge in the $VACF(-)$ for $Mt=0.5$ (Figure 5a), and is clearly apparent for $Mt=1.0$ (Figure 5b). This can be explained in terms of the coherent motion of a highly charged negative ion, and the positive ions surrounding it. The coherent motion in this range of concentration results in an increased persistence of velocity of the negative ions. Because the cluster tends to move coherently over a period of time longer than the mean collision time between ions in the cluster, this collective motion conducts the negative ion in the direction of the net drift of the entire cluster. In the cases presented in Figures 5a and 5b, the bump in the $VACF(-)$ is located at nearly twice the mean collision time between negative and positive particles. This fact suggests that the mechanism responsible for this velocity persistence is a double collision. First, a collision occurs between the negative central ion and the positive ions in front of it. Then, a second collision occurs when the same negative ion is reached by the positive ions which the electrostatic attraction drag behind it. In contrast, as seen in Figure 5c, these bumps are reduced at the higher concentration of $Mt=6.0$. In this case, there is perhaps not enough free volume for the ionic clusters to move coherently over appreciable distances.

In the previous MD simulations [8] for the 1-1 electrolytes, the modified Enskog theory of hard-sphere was shown to predict the self-diffusion coefficients

reasonably accurately. It is also interesting to note that the diffusion constants of positive ions for the 1-3 electrolytes here (Table 1) are close to those for the 1-1 electrolytes except for the low concentration limit of $Mt < 0.2$. However, the self-diffusion coefficients of negative ions are smaller by a factor of two or three than those of positive ions. An interpretation of this observation is that the free motion of negative ions is likely to be restricted by the formation of ionic aggregates.

For a hard-sphere system [26], the collision frequencies, ω_{ij} , are expressed in terms of the contact values of pair distribution functions,

$$\omega_{ij} = 4n_i d^2 (\pi kT/m)^{1/2} g_{ij}(d), \quad (6)$$

where ω_{ij} is the number of collisions per particle of component j , per unit time between particles of component i and j . The collision frequencies determined from the MD simulation are plotted in Figure 6. For the purpose of comparison with the corresponding hard-sphere system, the predictions using the MD contact values in eq. (6) are also shown in this figure. The MD results are seen to be in excellent agreement with theory. This suggests that the microscopical behavior of the primitive electrolytes is much like to the hard-sphere dynamics. In this sense, the transport properties of the primitive model electrolytes are, at least qualitatively, related to those for the system of hard-sphere fluids.

4. Conclusion

In the present paper we have reported the MD simulations for the thermodynamic and transport properties of 1-3 electrolyte solutions. The results obtained from computer simulations have been used to assess the applicabilities of theoretical equations, namely, the exponential form of Debye-Huckel theory, the mean spherical approximation, and the hypernetted chain theory. The HNC theory is shown to be the best approximation compared with the simulation results both for energy and for osmotic pressure. For asymmetrically charged 1-3 bulk electrolytes, the presence of ionic clustering was observed in pair distribution functions. The local maximum in g_{--} was shifted to $r = 2.5d$.

The MD results indicate that the diffusion processes are strongly dependent on concentration and the solvent have a negligible effect on the dynamics of solute ions. However, experimental diffusion coefficients in aqueous solutions [27] are nearly concentration independent. Under certain conditions the primitive model is known to be a realistic description for molten salts. One important aspect neglected in the primitive model electrolytes is the structural changes of the solvent according to the local concentration of solute ions. This simple model is inadequate to describe the ionic structures and dynamics in aqueous electrolyte solutions. With the complicated vibrational and orientational motions of water molecules, numerous factors are involved to ascertain the principal features governing the transport properties of aqueous solutions. Consequently, the satisfactory model potentials describing the detailed ionic motions in aqueous solutions are required for further work.

Acknowledgments

The Minnesota Supercomputer Institute supported this research with a computer grant and a fellowship to one of us (SHS).

References

- [1] C.W. Outhwaite, in: Statistical Mechanics Vol. 2, Specialist Periodical Reports, ed. K. Singer (The Chemical Society, London, 1975).
- [2] H.L. Friedman and W.D.T. Dale, in: Modern Theoretical Chemistry Vol. 5, Statistical Mechanics, ed. B.J. Berne (Plenum Press, New York, 1977).
- [3] E. Waisman and J.L. Lebowitz, J. Chem. Phys., **56** (1972) 3086, 3093.
- [4] J.C. Rasaiah and H.L. Friedman, J. Chem. Phys., **48** (1968) 2742; J.C. Rasaiah, *ibid.* **56** (1972) 3071.
- [5] H.C. Andersen, D. Chandler and J.D. Weeks, J. Chem. Phys., **57** (1972) 2626.
- [6] T.L. Croxton and D.A. McQuarrie, J. Phys. Chem., **83** (1979) 1840.
- [7] M. Medina-Noyola, D.A. McQuarrie and W. Olivares, Chem. Phys. Lett., **58** (1978) 351; M. Medina-Noyola, J. Chem. Phys., **81** (1984) 5059.
- [8] D.M. Heyes, Chem. Phys., **69** (1982) 155.
- [9] D.N. Card and J.P. Valleau, J. Chem. Phys., **52** (1970) 6232; J.P. Valleau and K. Cohen, J. Chem. Phys., **72** (1980) 5935; J.P. Valleau, K. Cohen and D.N. Card, J. Chem. Phys., **72** (1980) 5942.
- [10] W. van Megen and I. Snook, Molec. Phys., **39** (1980) 1043.
- [11] S.A. Rogde and B. Hafskjold, Molec. Phys., **48** (1983) 1241.
- [12] S. Ciccariello and D. Gazzillo, Molec. Phys., **48** (1983) 1369.
- [13] D. Levesque, J.J. Weis and J.P. Hansen, in: Topics in Current Physics Vol. 36, Applications of the Monte Carlo Method in Statistical Physics, ed. K. Binder (Springer, Berlin, 1984).
- [14] B.C. Freasier, Molec. Phys., **39** (1980) 1273.
- [15] P. Debye and E. Huckel, Physik Z., **24** (1923) 195, 305.
- [16] D.J. Adams, J. Chem. Phys., **78** (1983) 2585; D.J. Adams and G.S. Dubey, J.

- Comp. Phys., **72** (1987) 156.
- [17] P.P. Ewald. Ann. Phys. Leipzig, **64** (1921) 253.
- [18] M.J.L. Sangster and M. Dixon, Adv. Phys., **25** (1976) 247.
- [19] B.J. Alder and T.E. Wainwright, J. Chem. Phys., **31** (1959) 459.
- [20] W.J. McNeil and W.G. Madden. J. Chem. Phys., **76** (1982) 6221.
- [21] D.M. Heyes and L.V. Woodcock, Molec. Phys., **59** (1986) 1369.
- [22] L. Verlet, Phys. Rev., **159** (1967) 98.
- [23] H.J.C. Berendsen, J.P.M. Postma, W.F. van Gunsteren, A. DiNola and J.R. Haak, J. Chem. Phys., **81** (1984) 3684.
- [24] B.J. Alder, D.M. Gass and T.E. Wainwright, J. Chem. Phys., **53** (1970) 3813.
- [25] J.P. Hansen, F. Joly and I.R. McDonald, Physica, **132A**(1985) 472.
- [26] S. Chapman and T.G. Cowling, The Mathematical Theory of Non-Uniform Gases (Cambridge Univ. Press, 1970).
- [27] H.J.V. Tyrrell and K.R. Harris, Diffusion in Liquids. A Theoretical and Experimental Study (Butterworths, London, 1984).

Table 1. System characteristics and MD results
for 1-3 Primitive Model Electrolytes

Mt (moles/l)	-U/NkT	PV/NkT	D ₊ (10 ⁻⁴ cm ² /s)	D ₋ (10 ⁻⁴ cm ² /s)	ω_{++} (10 ¹⁰ s ⁻¹)	ω_{--} (10 ¹⁰ s ⁻¹)	ω_{-+} (10 ¹⁰ s ⁻¹)
0.02	0.5169 (0.0437)*	0.8558	315.21	113.84	0.068	0.000	1.929
0.2	1.1983 (0.0543)	0.7433	57.42	22.26	1.042	0.000	11.119
0.5	1.5010 (0.0495)	0.7239	28.54	12.94	2.801	0.000	17.185
1.	1.7423 (0.0495)	0.7370	17.24	8.817	5.977	0.007	23.603
2.	2.0022 (0.0469)	0.8110	9.574	5.553	13.142	0.014	33.174
4.	2.2978 (0.0438)	1.0293	5.151	3.288	31.182	0.019	50.895
6.	2.4957 (0.0405)	1.3495	3.490	1.699	55.679	0.167	70.319

* The values in parentheses indicate uncertainties in the MD simulations.

Figure Captions

1. Schematic of the molecular dynamics procedure.
2. Reduced configurational energy of 1-3 primitive model electrolytes as a function of concentration. \square MD results; — DHX; ----- MSA; - · - HNC[4].
3. Reduced osmotic pressure of 1-3 primitive model electrolytes as a function of concentration. The symbols have the same meaning as in Figure 2.
4. Pair distribution functions for like-pairs and unlike-pairs. (a) $Mt = 0.2$; (b) $Mt = 4.0$. Also shown as dotted curves are DHX predictions.
5. Normalized velocity autocorrelation function vs. time at three different concentrations: a) $Mt = 0.5$, b) 1.0, and c) 6.0. The solid curves correspond to the velocity autocorrelation function of positive ions ($VACF(+)$) and dotted curves to that of negative ions ($VACF(-)$).
6. Semilogarithmic plot of collision frequency as a function of concentration. \square MD results for ω_{++} ; \blacksquare MD results for ω_{-+} . The dotted curves are predictions by Eq. (6) using the MD contact values of pair distribution functions.

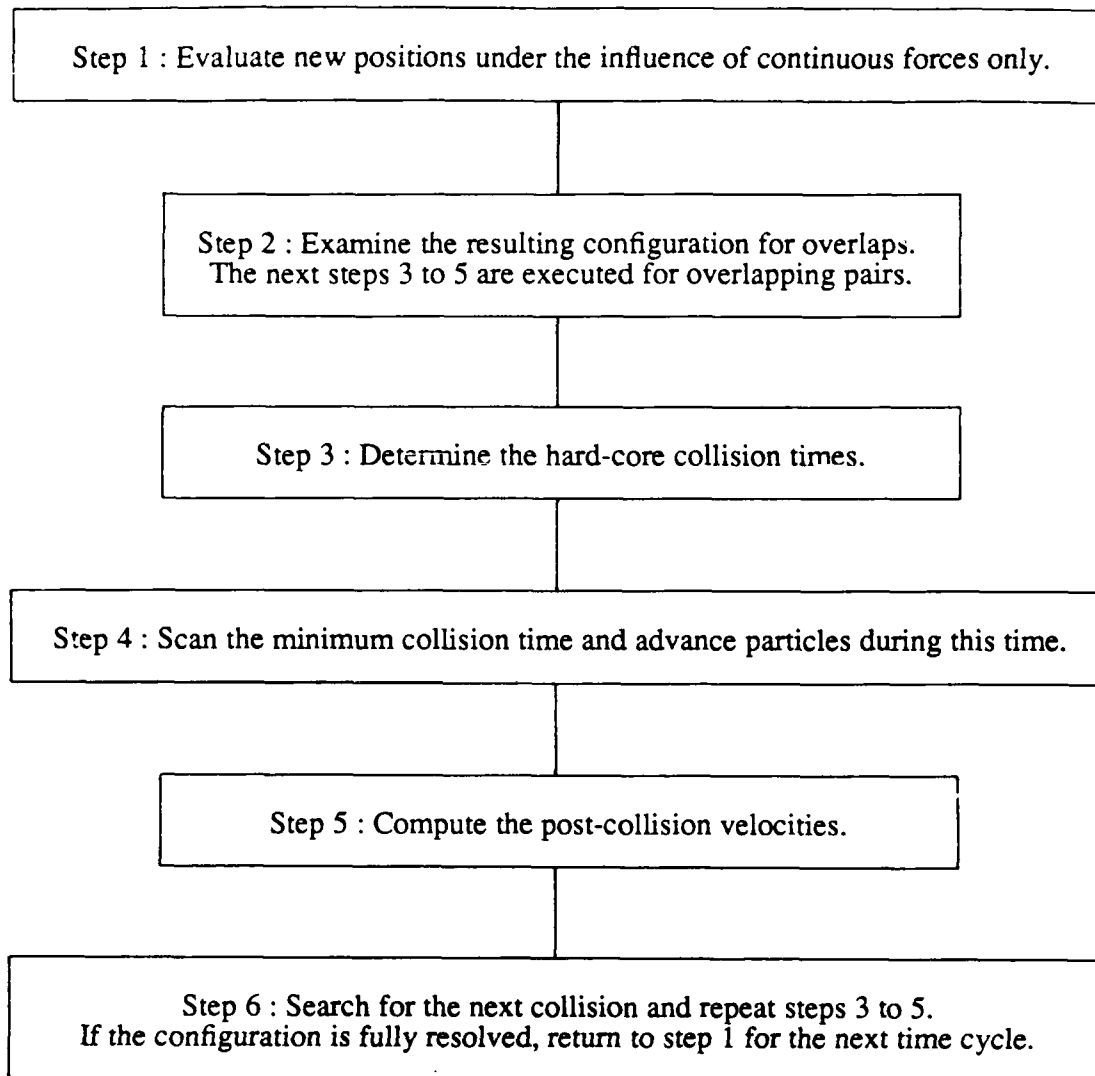


Fig 1. Suh et al.

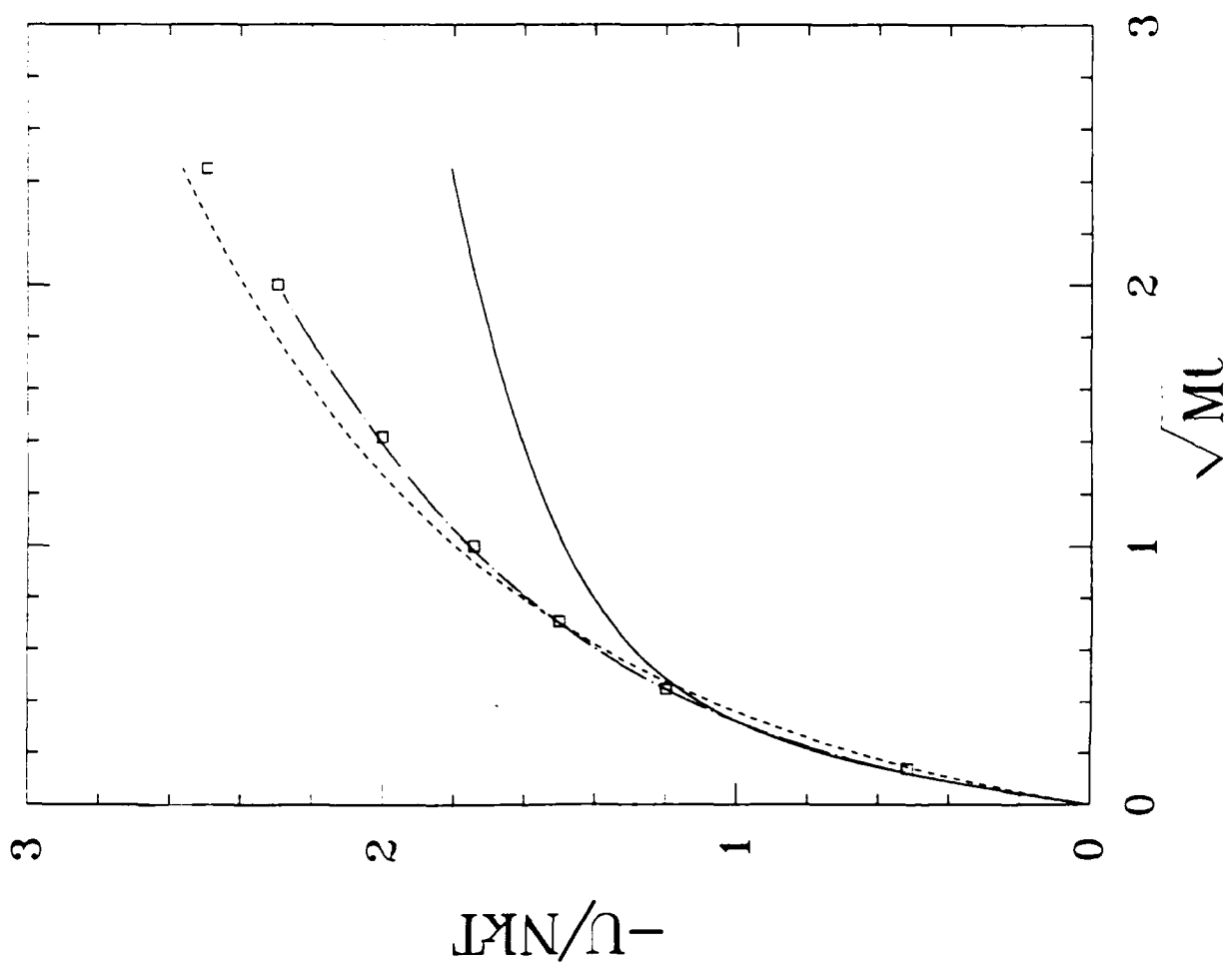


Fig 2 Sub et al.

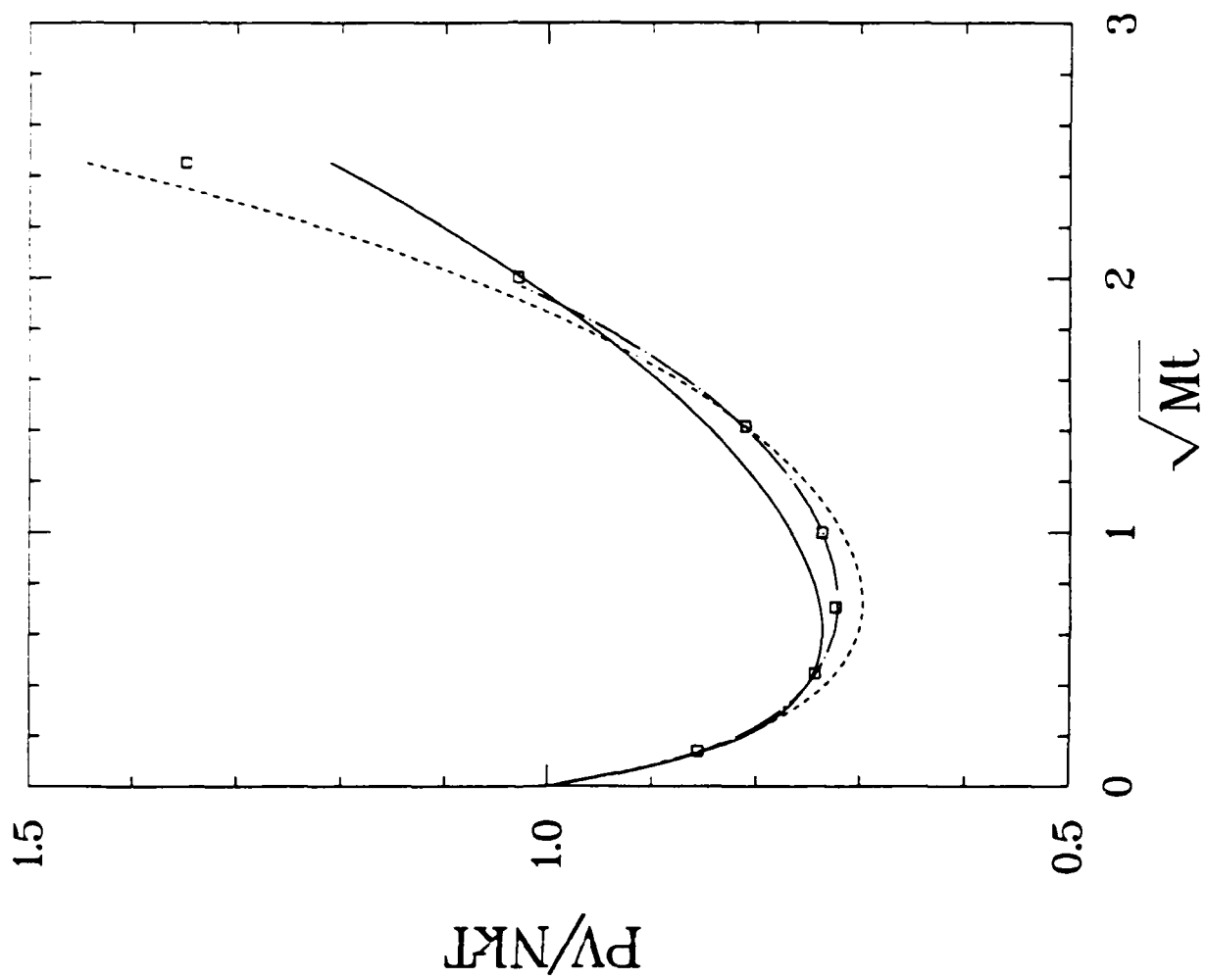


Fig. 3 Sub et al.

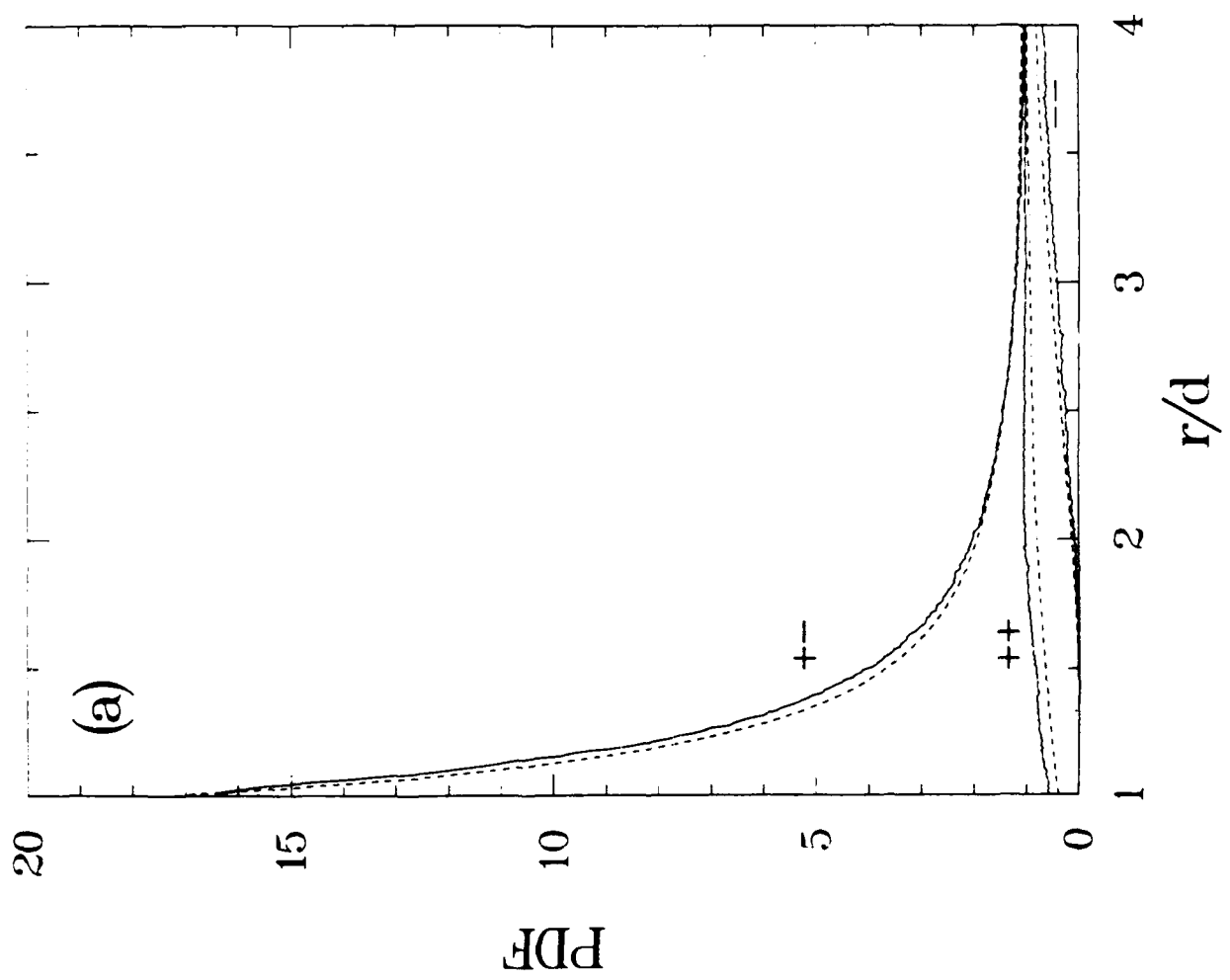


Fig 4(a) Sub of a.

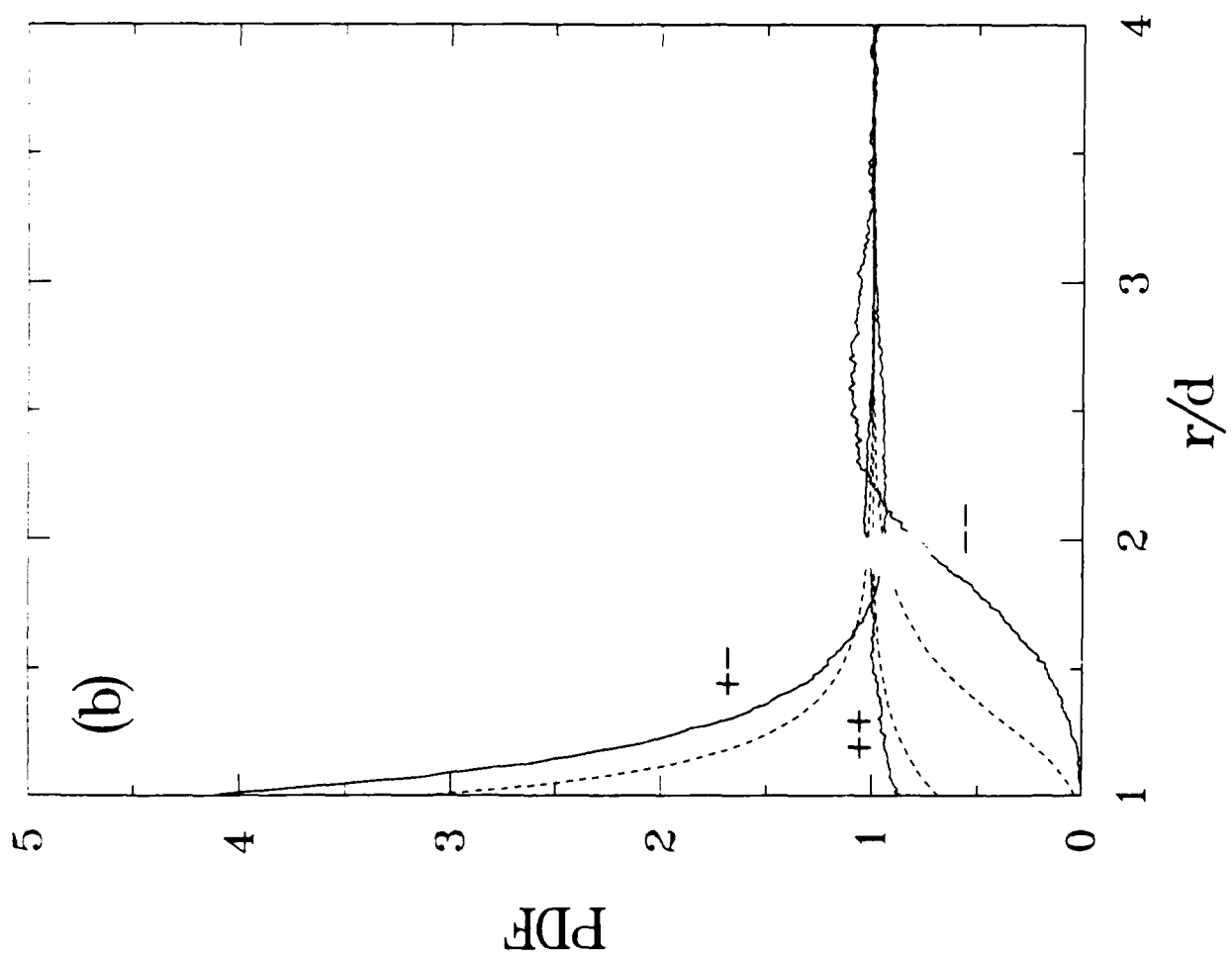


Fig 4(b) Suh et al.

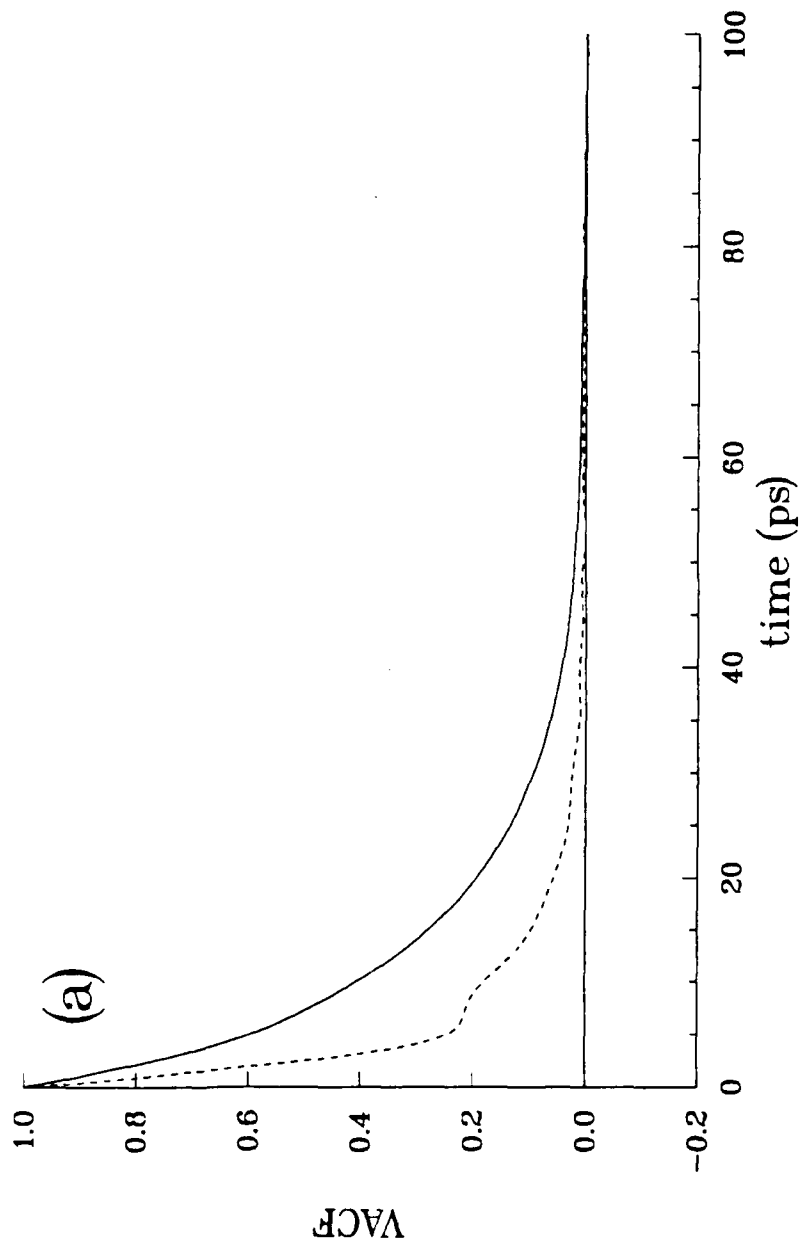


Fig 5(a) sub d d

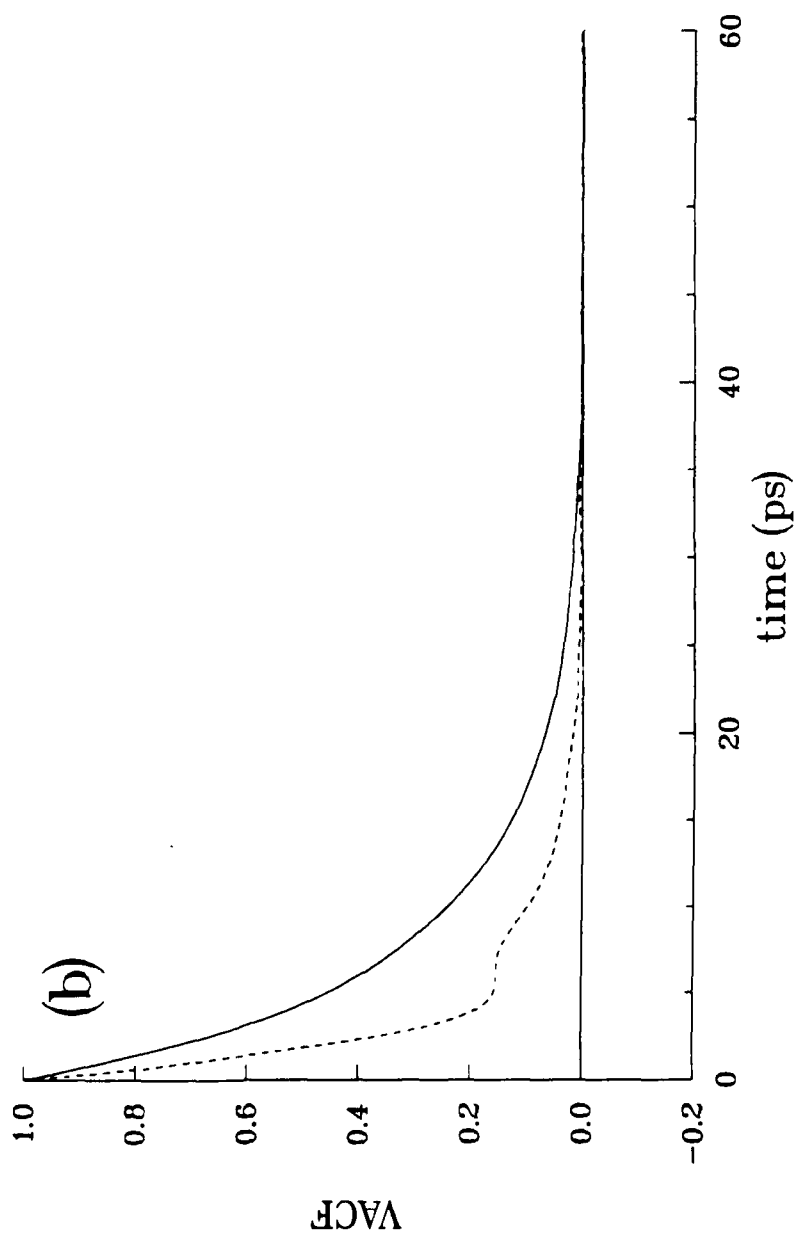


Fig 5(b) Sub of a.

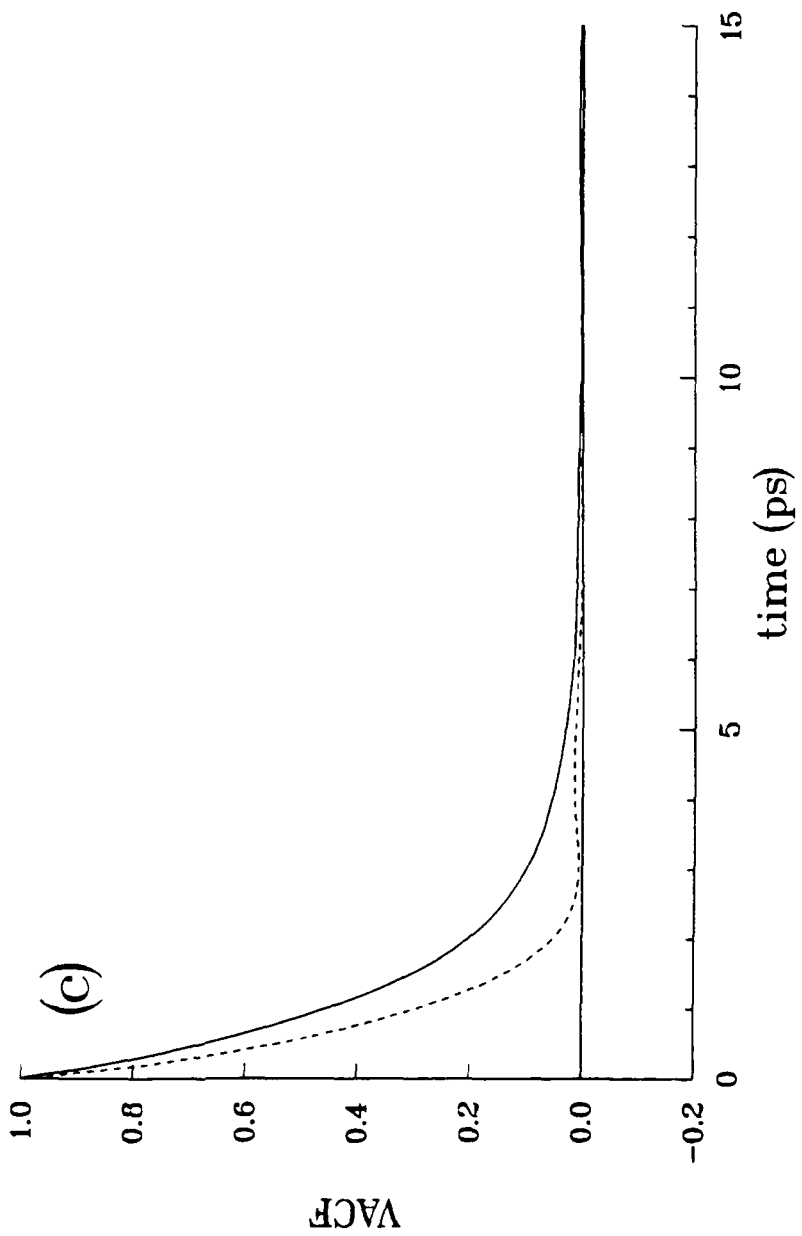


Fig 5(c) Sub d u

Fig 6 Sub et al.

